Sea spray aerosol organic enrichment, water uptake and surface tension effects (supplement)

Luke T. Cravigan[1], Marc D. Mallet[1,a], Petri Vaattovaara[2], Mike J. Harvey[3], Cliff S. Law[3,4], Robin L. Modini[5,b], Lynn M. Russell[5], Ed Stelcer[6,c], David D. Cohen[6], Greg Olsen[7], Karl Safi[7], Timothy J. Burrell[3], and Zoran Ristovski[1]

[1]International Laboratory for Air Quality and Health, CPME, Queensland University of Technology, Brisbane, Australia
[a]Now at Defence Science and Technology Group, Melbourne, Australia
[2]University of Eastern Finland, Kuopio, Finland
[3]National Institute of Water and Atmospheric Research, Wellington, New Zealand
[4]Department of Marine Sciences, University of Otago, Dunedin, NZ
[5]Scripps Institute of Oceanography, University of California, San Diego, La Jolla, California
[b]Now at Laboratory of Atmospheric Chemistry, Paul Scherrer Institute, 5232 Villigen PSI, Switzerland
[6]Centre for Accelerator Science, NSTLI, Australian Nuclear Science and Technology Organisation, Menai, NSW, Australia
[c]Deceased
[7]National Institute of Water and Atmospheric Research, Hamilton, New Zealand

Correspondence: Zoran Ristovski (z.ristovski@qut.edu.au)

1 Seawater samples

Table S1 provides a description of the seawater samples taken to generate SSA during the SOAP voyage. The pre-selected particle mobility diameter selected for the VH-TDMA volatility profiles and the samples for which filters were collected are also shown in Table S1.

2 Seawater analyses

2.1 Chlorophyll a and phytoplankton

Chlorophyll a concentration was measured by filtering 2 litres of sample water onto GF/F Whatman filters, with immediate freezing in liquid nitrogen and subsequent analysis within 3 months of collection. Filters were ground and chlorophyll a extracted in 90 % acetone with concentration determined by a calibrated fluorometer (Perkin-Elmer), with an analytical precision of $0.001\,\mathrm{mg\,m^{-3}}$ (Law et al., 2011). Phytoplankton speciation, abundance and Carbon were determined by optical microscopy of samples preserved in Lugol's solution (Safi et al., 2007).

Table S1. Details of ocean water samples collected for generation of SSA.

Water sample	Depth [m]	Depth class	Date/Time [UTC+12]	Bloom	Lat/Lon [S/E]	Chl a [g/L]	D (VH-TDMA) [nm]	Filter
Workboat 1	0.1	Surface	15/2/12 8:05	1	44.621/174.772	0.985	50	Y
Workboat 4	0.1	Surface	17/2/12 8:02	1	44.587/174.690	1.405	50	Y
CTD U7505	50	Deep	18/2/12 9:16	1	44.574/174.735	0.974	50	Y
Workboat 5	0.1	Surface	18/2/12 8:04	1	44.590/174.685	1.160	50	Y
CTD U7506	2.79/505.5	Mixed/Deep	19/2/12 7:30	-	44.335/175.246	0.91/-	50	Y
CTD U7507	4.09	Mixed	20/2/12 7:15	-	45.960/173.646	0.880	50/100	N
CTD U7508	2.07/400	Mixed/Deep	21/2/12 7:55	-	43.741/176.966	0.670/- 7 50	N	
CTD U7510	3.13	Mixed	22/2/12 9:22	2	43.717/-178.156	1.520	50	Y
Workboat 6	0.1	Surface	22/2/12 8:27	2	43.715/-179.860	1.530	50	Y
Workboat 7	0.1	Surface	24/2/12 13:03	2	43.585/-179.753	0.490	50	Y
CTD U7518	254.7	Deep	24/2/12 15:15	2	43.599/-179.767	-	30/50	Y
CTD U7520 [a]	211.62	Mixed	25/2/12 14:30	2	43.630/179.741	0.630	50	Y
CTD U7521	2.48	Mixed	26/2/12 6:52	-	43.962/179.308	-	50	Y
Workboat 8	0.1	Surface	27/2/12 14:39	3a	44.110/175.140	0.530	50/100	Y
CTD U7524	11.21	Mixed	28/2/12 13:10	3a	44.542/174.873	0.460	50	Y
Workboat 9 [b]	30.1	Surface	29/2/12 8:03	3a	44.600/174.870	0.290	50/130	Y
CTD U7528	9.17	Mixed	2/3/12 14:59	3b	44.191/174.944	0.450	50	Y
CTD U7530	10.31/810.5	Mixed/Deep	3/3/12 14:45	3b	44.781/174.650	0.490/-	50	Y
CTD U7532	8.96	Mixed	4/3/12 15:25	3b	44.243/174.523	1.010	50	Y
Workboat 10	0.1	Surface	5/3/12 9:04	3b	44.185/174.295	-	50	Y

[a] Thermodenuder placed upstream of H-TDMA and UFO-TDMA. No VH-TDMA organic fractions available. [b] DRH measured for Workboat 9.

2.2 Fatty Acids and Alkanes

Oasis hydrophillic-lipophillic balance (HLB) solid phase extraction (SPE) cartridges (6 ml; 150 mg) were rinsed with 2 mL acidified nano-pure water before eluting with 2 x 1 mL methanol followed by 1 x 1 mL (1:1; v/v) methanol:dichloromethane. The solvent extract was concentrated to dryness using a LABCONCO RapidVap dry nitrogen evaporation system at 40 °C. Extracts were reacted with 5% boron trifluoride (BF3) in methanol for 20 min at 70 °C to generate the methyl ester or ether derivatives of carboxylic acids and alcohols respectively (Simoneit, 2004; Fu et al., 2008, 2010). Fatty acid methyl esters (FAMEs) and n-Alkanes were partitioned into a mixture of hexane:dichloromethane (2:1; v/v) and evaporated to dryness under nitrogen. The final volume was adjusted to 0.5 mL using dichloromethane following the addition of C17:0 FAME internal standard and stored at -20 °C. Gas chromatography-mass spectrometry (GC-MS) analyses of n-Alkanes and derivatized FAME samples were performed on an Agilent 6890N GC and 5975B Mass Selective Detector (MSD) fitted with a split/splitless

injector and CTC PAL auto-sampler. FAME and n-Alkanes were analysed using a polar ZB-WAX fused-silica column (30m x 0.25 mm ID, 0.25 µm film thickness, Phenomenex). The GC operating conditions for FAMES were as follows: temperature hold at 55 °C for 2 min, increase from 55 to 150 °C at 10 °C min^{-1}, increase from 150 to 240 °C at a rate of 1.8 °C min^{-1} with final isothermal hold at 240 °C for 5 min. Helium was used as carrier gas at flow rate of 1.5 mL min. The sample was injected in splitless mode with the injector temperature at 240 °C. Mass spectra were acquired and processed using Agilent Chemstation Software with the MSD operated in full scan electron ionization (EI) mode (70 eV) with mass range 50-450 amu; solvent delay 6.2 min. MSD operating conditions were: electron multiplier 1700-1800 V; transfer line 250 °C; MS Source 250 °C; MS Quad 150 °C; autotune file PFTBA normalized. The GC operating conditions for Alkanes was similar to parameters described for FAMES above except the final temperature was 250 °C with final isothermal hold at 250 °C for 5 min, injector temperature of 250 °C, MSD mass range 50-500 amu and solvent delay of 5.8 min. Identifications were confirmed by comparison of mass spectra with those of previously reported spectra, and by comparison of retention data with data obtained for commercial laboratory standards and interpretation of mass spectrometric fragmentation patterns. GC-MS response factors were determined using authentic standards. Quantification was conducted using calibration curves by analysing aliquots of a stock solution of Supelco FAME Mix (C8:0 to C24:1) or n-Alkane standards (n-C14 to n-C36). Quantitative recovery was checked with an n-alkane mixture (n-C14 to n-C36) and FAME Supelco Mix (C8:0 to C24:1). Recoveries of standards were generally better than 80% except for C20:4 n-6 and C22:6 n-3 polyunsaturated compounds. Blank SPE cartridges were analyzed by the procedure used for the real samples. The results showed that the contamination levels were less than 2% of real samples for most compounds except for the n-alkanoic acid homologues (C14:0, C16:0 and C18:0) which could be as high as 5%.

2.3 High-molecular-weight reducing sugars and proteins

Somogyi:1926te, Nelson:1944wh, Hartree:1972uc, Somogyi:1952te, Lowry:1951vb, burrell2015bacterial Other organic parameters sampled included High Molecular Weight reducing sugars and Proteins (Somogyi, 1926, 1952; Burrell, 2015), and CDOM (Liquid Waveguide Capillary Cell, Gall et al. (2013)). High-molecular-weight (HMW) reducing-sugar concentration was quantified using the Somogyi-Nelson detection method in conjunction with filtration (Somogyi, 1926). A minimum of 150 mL of sample seawater was filtered through a 25 mm glass-fibre filter (GF/F - Whatman), following filtration each filter was stored in a 5 ml flat base polypropylene vial (Sarstedt) and frozen at -20 ° C until post cruise laboratory analysis. Using aseptic techniques, each sample filter was defrosted and cut into twelve individual pieces following a standardised cutting pattern. Appropriate reagents were added in accordance with Nelson (1944), and sample filters were then heated in a water bath at 100 ° C for 15 min. A linear six-point glucose calibration curve (0 to 300 µg mL^{-1}) incorporating blank GF/F filters was also prepared in triplicate. Final solutions were centrifuged at 13 000 x g for 1 min to pelletise any loose glass-fibre filter strands, then 200 µL aliquots of each sample was placed in a clear flat bottom 96 well tissue culture plate (Sarstedt). Sample absorbance was measured at 520 nm wavelength on a plate reader at 25 ° C (SpectraMax190-Molecular Devices). Calculated sample concentrations were converted to µg mL^{-1} based on the original volume of seawater filtered. Using the reference glucose standard curve, final HMW reducing-sugar concentrations reflect glucose equivalent values. The sensitivity of this methodology is estimated at a maximum detection of 0.6 mg and minimum detection of approximately 0.01 mg (Somogyi, 1952; Burrell,

2015). HMW protein concentration was quantified using the Modified Lowry method in conjunction with filtration (Lowry et al., 1951; Hartree, 1972). Each sample was collected following the same methodology described for HMW reducing-sugar detection. Reagent preparation and standard sample analysis protocol were modified from Hartree (1972). A six point linear Bovine Serum Albumin (BSA) protein calibration curve (0 to 1000 $\mu g\,mL^{-1}$) was run in triplicate with blank GF/F's directly

5   incorporated. As described for HMW reducing sugars, HMW protein concentration samples were centrifuged at 13 000 x g for 1 min prior to absorbance determination at 560 nm wavelength using a 96 well plate reader at 25 °C (SpectraMax190-Molecular Devices). This analytical technique is capable of detecting dipeptides, with the detection efficiency increasing with increasing peptide size. The working detection limit is thought to be approximately 5 to 2000 $mg\,mL^{-1}$ (Hartree, 1972).

3   Seawater molecular classes

10   The OCEANFILMS model was implemented for the surface and mixed layer nascent SSA experiments with measured water parameters used to represent bulk seawater molecular classes. The distribution of molecular classes in the seawater samples was generated assuming that:

- the lipid class concentration was equal to the seawater total concentration of fatty acids,

- the protein class concentration was equal to the seawater total high molecular weight proteins,

15   - the polysaccharide class concentration was equal to the seawater high molecular weight reducing sugars,

- the processed molecular class concentration was assumed to make up the remainder of the DOC, and

- the humic like class concentration was assumed to be zero, because only surface and mixed layer measurements were taken used.

Note that the seawater measurements were not micro layer measurements, however the seawater samples were collected via

20   CTDs or on workboats and therefore probably don't represent the SML. Missing water composition data were filled using the relationships outlined in Burrows et al. (2014), based on the lifetime of each molecular class, for example the bulk concentration of proteins was assumed to be equal to one third of the polysaccharide concentration, when no other data were available. The processed molecular class concentration was assumed to make up the remainder of the DOC after polysaccharides, proteins and lipids have been subtracted, a minimum was applied to the concentration of processed compounds to prevent unrealistically

25   low or negative concentrations. The langmuir adsorption coefficients for each molecular class was taken directly from Burrows et al. (2014). OCEANFILMS was run including the co-adsorption of polysaccharides with all other molecular classes (Burrows et al., 2016), and an assumed bubble thickness of 0.3 μm. Figure S1 shows the distribution of the molecular classes in the seawater samples that were used as input to OCEANFILMS.
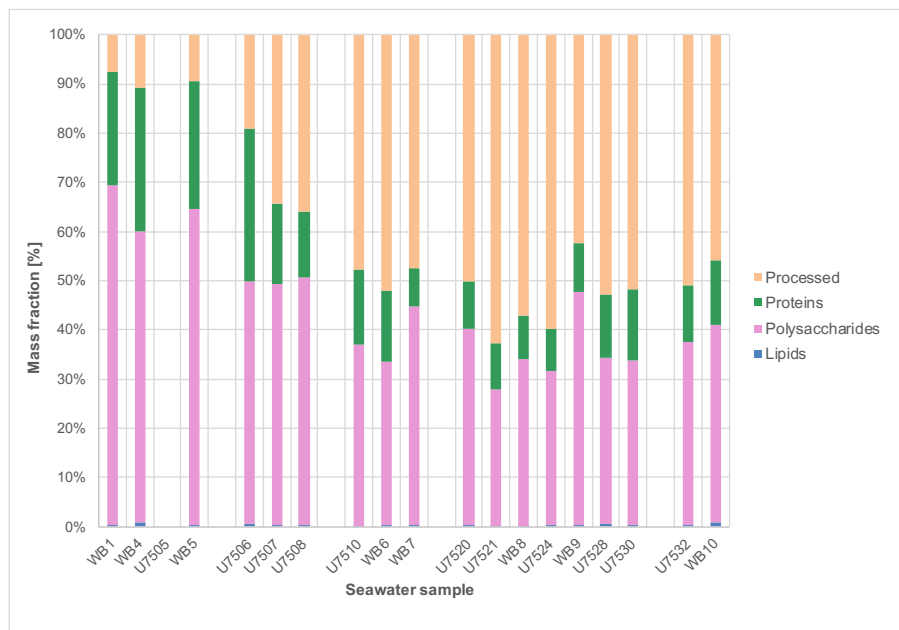
Figure S1. Distribution of organic functional groups in seawater samples used to generate SSA.

4   SSA organic fraction from volatility

The relationship between the volatility of laboratory sea salt (without an organic component) and sea spray generated from natural seawater samples was used to determine the sea spray organic volume fraction as described in the text. The organic volume fraction was inferred from volatility measurements using the linear model outlined in Eq. 1, where VF_T is the measured

5   volatile fraction of the sea spray sample at thermodenuder temperature T and $VF_{T,SS}$ is the measured volatile fraction of laboratory sea salt at temperature T. Figure S2 shows the volatile fraction of the SSA generated from each of the seawater samples and the volatile fraction of the laboratory sea salt as a function of temperature. The linear fits for each of the samples is also shown.

    The linear model was primarily computed over the temperature range 250 - 400 °C, over which it was assumed that only

10 hydrates evaporated for the SSA sample, based on reported volatility profiles of nascent SSA generated from natural seawater and from laboratory sea salts (Modini et al., 2010b; Rasmussen et al., 2017). For some samples measurements didn't cover the temperature range 250 - 400 °C, and therefore the fit was computed for slightly different values as shown in Table S2. The proportion of volatility due to sea salt components (hydrates) in the natural SSA sample (relative to laboratory sea salt) is given by f and is computed from the slope of Eq. 1. The proportion of the volatility due to sea salt hydrates, f, was assumed to

15 represent the proportion of sea salt in the natural SSA sample, and therefore $1 - f$ provided the fraction of total organics. For example an internally mixed SSA particle with an organic volume fraction of 50% and a sea salt (including hydrate) volume fraction of 50% has half the volume of hydrates compared the laboratory sea salt particles of the same diameter. The volatility
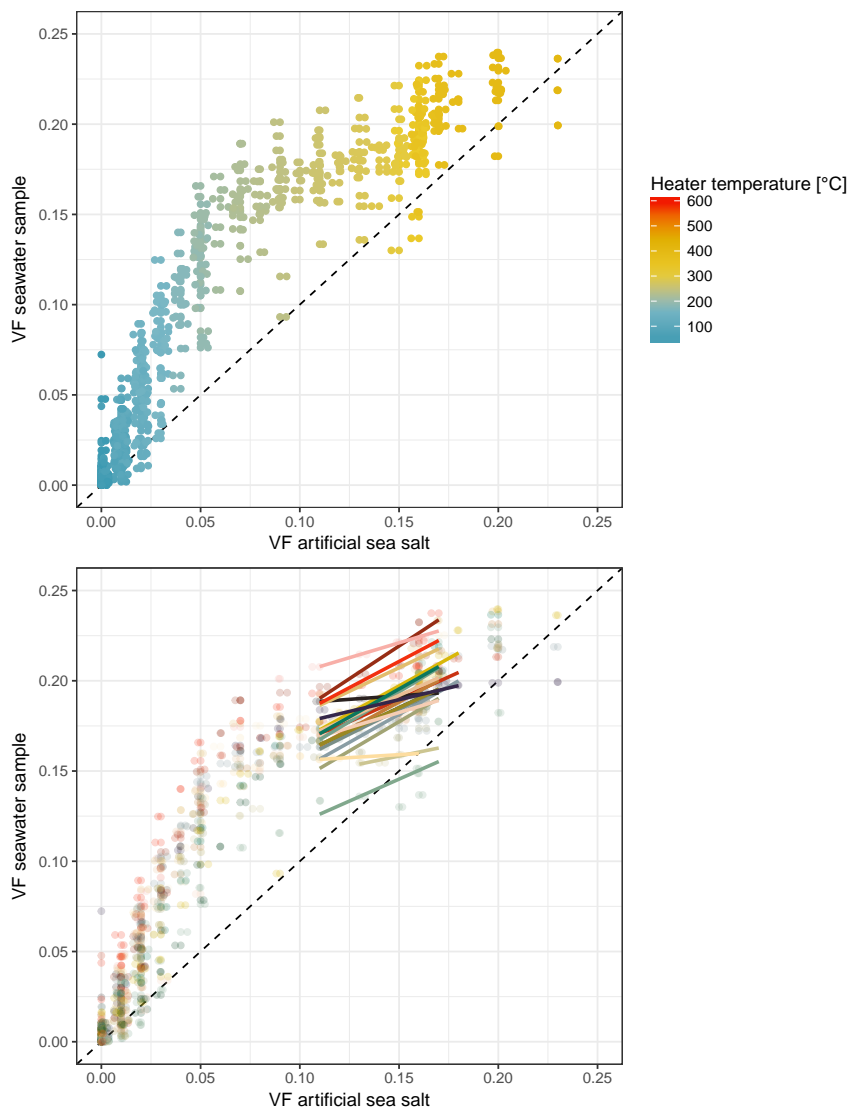
Figure S2. Volatile fraction (VF) for SSA generated from laboratory sea salt and natural seawater. Coloured as a function of heater temperature (top) and by sample (bottom). Solid lines show the fitted linear model over 200 to 400 °C, dashed line shows VF from natural SSA equal to VF from laboratory sea salt.

due to hydrates will be reduced by half and therefore f will also be reduced by half, assuming that hydrates dominate the volatility at 200 - 400 °C. The concentration of semi-volatile organics (OVF_{sv}) was assumed to be equal to the intercept in Eq. 1, that is the excess volatility at temperatures less than 200 °C in the natural SSA relative to sea salt. The linear fits for
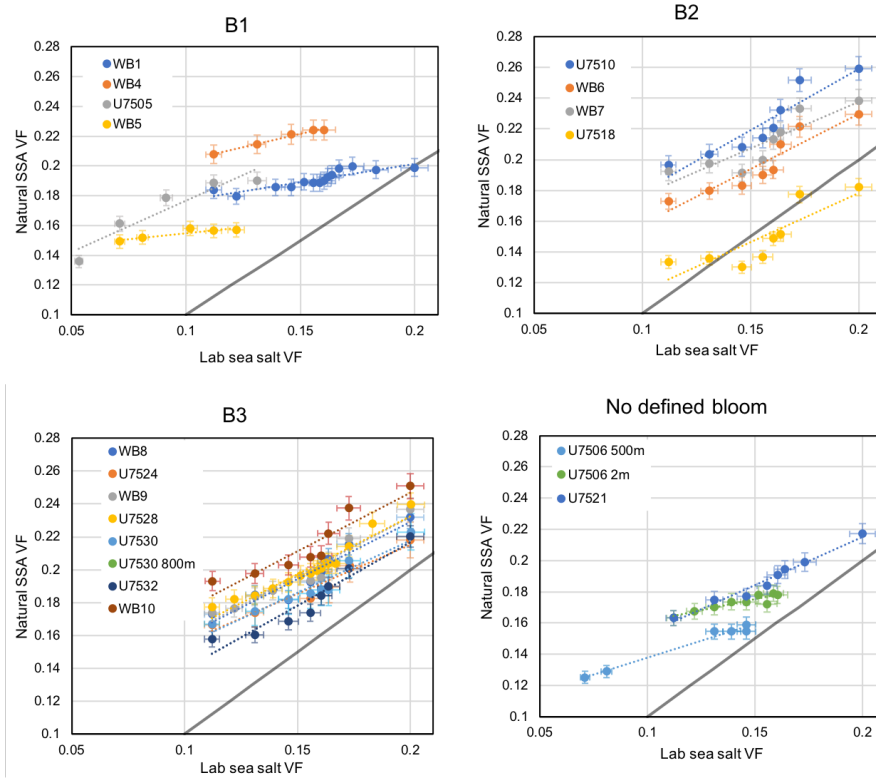
Figure S3. Linear fits of the volatile fraction of laboratory sea salt and natural sea spray aerosol for temperature range over which the organic fraction was calculated. Bloom 1 (B1) measurements shown on top-left, bloom 2 (B2) on top right, B3 on bottom left and measurements from outside defined bloom periods on the bottom right.

each sample are shown in detail in Figure S3 and Table S2 shows the slope (f) and intercept, the standard error in the slope and intercept and the R^2 values for the linear fit.

$$VF_{T=200-400°C} = f \times VF_{T=200-400°C,SS} + OVF_{sv} \tag{1}$$

5   The method used to compute the organic volume fraction implicitly assumes that the proportion of hydrates in the sea salt component of SSA is constant, however observations have shown variability in inorganic composition of SSA can vary (Salter et al., 2016; Schwier et al., 2017; Ault et al., 2013), particularly species such as Ca, Cl and Mg, which are potentially important for the formation of hydrates. As a result further correction was applied to f for the case where the profile of inorganic species, and therefore hydrates, is different between the natural SSA sample and the laboratory sea salt sample. The correction is

10   represented by f_{io} in Eq. 2. The ionic composition of nascent SSA generated from natural seawater was measured using ion beam analysis and used to compute the inorganic molecular composition, the AIOMFAC model (Zuend, 2019; Zuend et al.,

2008) was used to compute the molecular composition, using the mole fractions of Na, K, Mg, Ca, and Cl from ion beam analyses (for natural SSA samples) and from known composition (laboratory sea salt). The results from the IBA, which was used as input for AIOMFAC, and FTIR analyses are outlined in 5. The volume fraction of hydrates for each sample was subsequently computed assuming that the

5   - Sodium sulfate is in the form of a deca hydrate (with density $1.46 \ g \ cm^{-3}$)

    - Magnesium sulfate is in the form of a hepta hydrate (with density $1.68 \ g \ cm^{-3}$)

    - Calcium sulftae is in the form of a di hydrate (with density $2.32 \ g \ cm^{-3}$)

    - Magnesium chloride is in the form of a hexa hydrate (with density $1.57 \ g \ cm^{-3}$), and

    - Calcium chloride is in the form of a hexa hydrate (with density $1.71 \ g \ cm^{-3}$).

10   The above analysis was performed based on the ionic composition of laboratory sea salts and f_{io} was computed as the ratio of natural seawater SSA hydrate volume fraction to laboratory sea salt hydrate volume fraction. Densities were taken from Rumble (2018). Table S2 shows the hydrate volume fractions estimated from AIOFMAC and the resulting f_{io} values.

$$OVF_{tot} = 1 - \frac{f}{f_{io}} \qquad (2)$$

5   SSA water uptake

15   HGFs for sea salt were shape corrected using the dynamic shape factor from (Zieger et al., 2017). The presence of an organic fraction has been observed to increase the sphericity of nascent SSA (Laskin et al., 2012), therefore an organic fraction dependent shape correction was applied (Zelenyuk et al., 2007). A single shape factor was used across all temperatures because TEM images of laboratory sea salt showed an insignificant difference between the apparent shape of SSA at ambient temperature and those heated to 250 °C as shown in Figure S4.

20   The HGFs observed for SSA generated from both laboratory sea salt and natural seawater samples showed up to 3 externally mixed HGF modes. The first natural seawater SSA HGF mode averaged 1.89 ± 0.07 and contributed a number fraction of 0.8 ± 0.12 for 50 nm diameter SSA. The second mode displayed an average HGF of 2.04 ± 0.09 and contributed a number fraction of 0.2 ± 0.1. The third HGF mode was sporadically observed during SOAP measurements at 50 and 100 nm diameters (observed during 4 samples), when present contributed number fraction of 0.01 to 0.06 and displayed an average HGF of

25   2.25 ± 0.02. Figure S5 shows the difference in the HGF between the first HGF mode and the subsequent modes. The proportion of the second HGF mode at 100 nm, appears to be consistent with a greater contribution from the lognormal mode 3.

     The measured HGFs from the VH-TDMA for both heated and ambient temperature samples are shown in S6. Ambient temperature was defined as the average of all measurements less than 45°C, and heated was defined as the average HGF for all measurements between 255 - 405 °C. As described in the text the heated SSA display slightly higher HGF than unheated SSA,

Table S2. Statistics for the volatile fraction linear fits, as well as the hydrate volume fraction estimated from AIOFMAC and fio values.

Sample	Depth	f (slope)	OVF_{sv} (intercept)	f std err	Intercept std err	R^2	Temp. range (^{o}C)	SS hydrate volume fraction	f_{io}
WB1	surface	0.24	0.15	0.04	0.01	0.80	250 - 400	0.36	0.82
WB4	surface	0.36	0.17	0.02	0.00	0.99	250 - 350	0.34	0.78
U7505	50	0.69	0.11	0.14	0.01	0.89	200 - 280	0.35	0.81
WB5	surface	0.16	0.14	0.05	0.00	0.79	220 - 270	0.39	0.91
U7506	505.5	0.43	0.09	0.04	0.00	0.98	220 - 300	0.38	0.88
U7506	2.79	0.28	0.14	0.09	0.01	0.83	250 - 350	0.43	0.99
U7510	3.13	0.80	0.10	0.13	0.02	0.87	250 - 400	0.34	0.77
WB6	surface	0.72	0.09	0.12	0.02	0.87	250 - 400	0.45	1.04
WB7	surface	0.61	0.12	0.13	0.02	0.78	250 - 400	0.41	0.94
U7518	254.7	0.64	0.05	0.17	0.03	0.71	250 - 400	0.47	1.08
U7521	2.48	0.62	0.09	0.04	0.01	0.97	250 - 400	0.39	0.89
WB8	surface	0.64	0.10	0.24	0.04	0.70	280 - 360	0.38	0.87
U7524	11.21	0.60	0.10	0.01	0.00	1.00	250 - 400	0.36	0.84
WB9	surface	0.72	0.09	0.07	0.01	0.94	250 - 400	0.35	0.80
U7528	9.17	0.70	0.09	0.05	0.01	0.93	250 - 400	0.45	1.03
U7530	10.31	0.64	0.09	0.08	0.01	0.92	250 - 400	0.34	0.78
U7530	810.5	0.51	0.11	0.06	0.01	0.86	250 - 400	0.29	0.68
U7532	8.96	0.77	0.06	0.09	0.01	0.92	250 - 400	0.38	0.87
WB10	surface	0.71	0.10	0.11	0.02	0.87	250 - 400	0.41	0.93

which is consistent with the change in HGF observed for sea salt (Modini et al., 2010a). No significant correlation is observed between the HGF and the organic fraction (mass or volume).

The results for the compressed film model output for heated SSA are shown in Fig. S7. These results are very similar to that observed for the ambient SSA, with the error in modelled HGF displaying a large reduction when all of the organics are partitioned to the particle surface. The similarity between heated and unheated SSA samples suggests that the organic component is largely refractory.
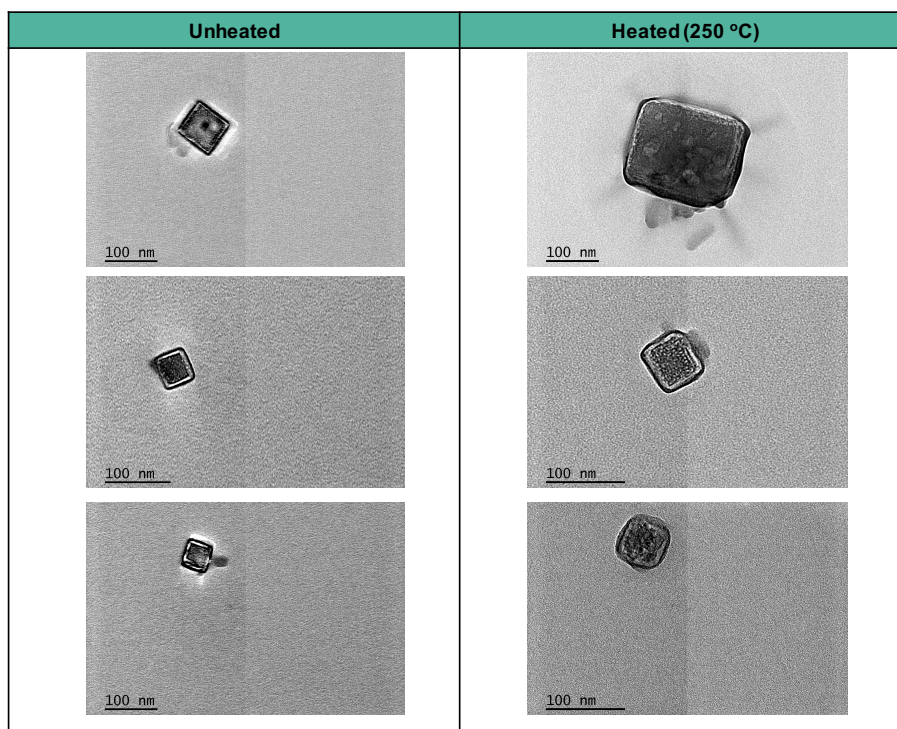
Figure S4. TEM images of laboratory sea salt particles collected at ambient temperature (left) and collected after heating to 250 °C (right). Typical samples selected. Unheated samples analysed approx. 1-2 hours after collection, heated samples analysed approx. 24 hours after collection.
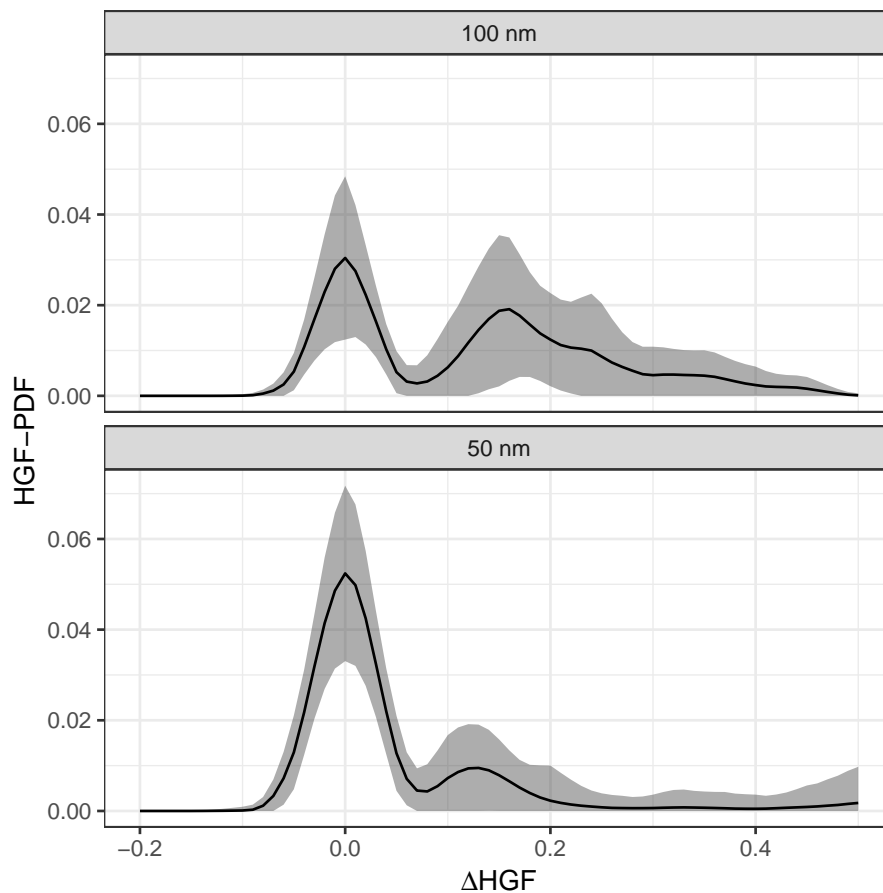
Figure S5. HGF modes for pre selected 100 nm diameter SSA (top) and 50 nm SSA (bottom) averaged across all natural SSA samples at ambient temperature. The x-axis has been shifted so that the mean of the first HGF mode is at 0. ΔHGF is the measured HGF minus the mean of the first HGF mode. HGFs are not Kelvin or shape corrected. The dark lines represent the average for all HGF distributions measured at that diameter and the shading is the standard deviation in the average.
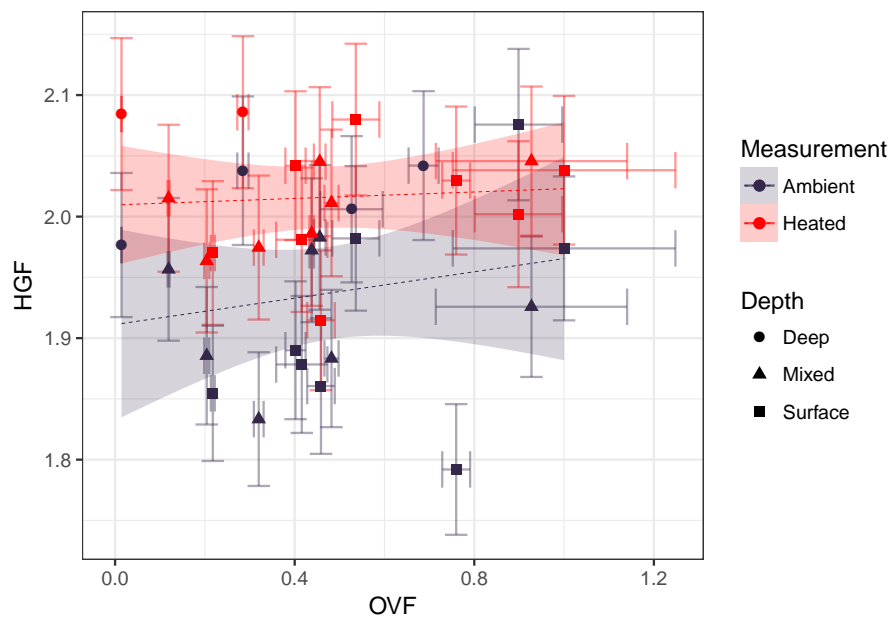
Figure S6. HGF as a function of organic volume fraction for ambient temperature (dark blue) and heated to 255 - 400 °C (red) measurements. Linear fit to both the heated and ambient measurements shown with dashed lines, shaded area represent the 95% confidence interval in the linear fit.
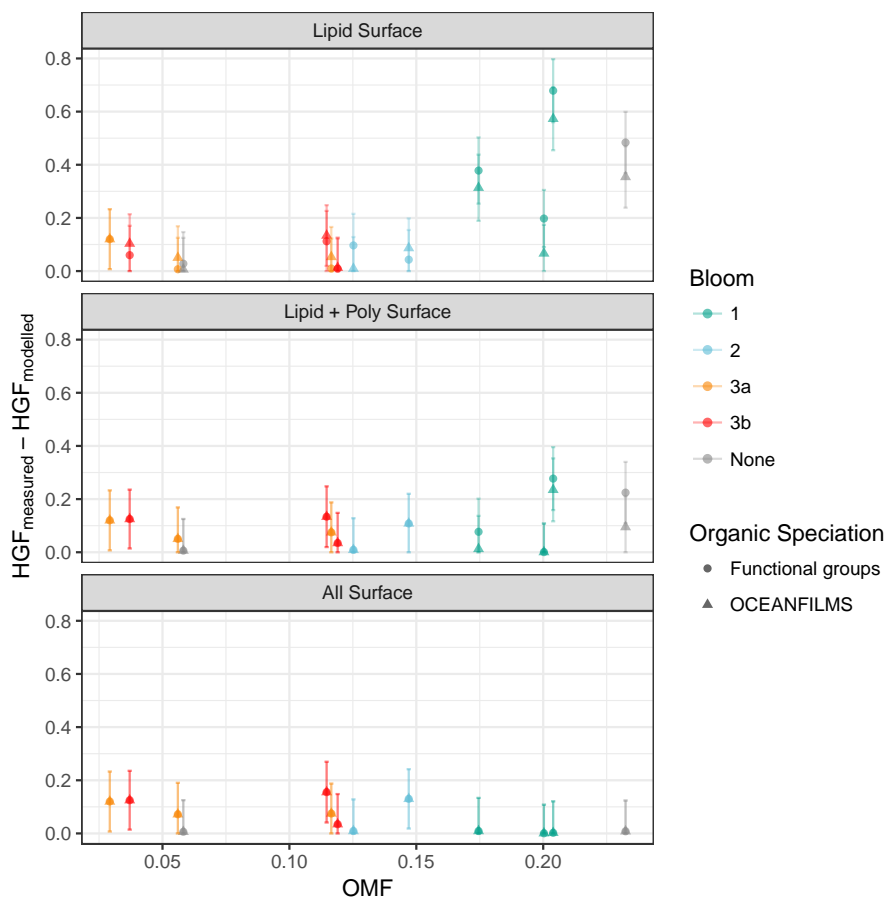
Figure S7. Compressed film mode heated HGF error (absolute value of measured minus modelled HGF) for lipids partitioned to the surface (top), lipids and polysaccharides partitioned to the surface (2nd panel from top), lipids polysaccharides and processed organics partitioned to the surface (2nd panel from bottom) and all organics partitioned to the surface (bottom). Organic speciation derived from FTIR measurements (circles) and from OCEANFILMS model (triangles). Compressed film model A_0 and V_{org} values were determined by those that resulted in the best fit between observed and modelled HGF for each sample.

References

Ault, A. P., Moffet, R. C., Baltrusaitis, J., Collins, D. B., Ruppel, M. J., Cuadra-Rodriguez, L. A., Zhao, D., Guasco, T. L., Ebben, C. J., Geiger, F. M., and et al.: Size-dependent changes in sea spray aerosol composition and properties with different seawater conditions, Environ. Sci. Technol., 47, 5603–5612, https://doi.org/doi: 10.1021/es400416g, 2013.

5 Burrell, T. J.: Bacterial extracellular enzyme activity in a future ocean, 2015.

Burrows, S. M., Ogunro, O., Frossard, A. A., Russell, L. M., Rasch, P. J., and Elliott, S. M.: A physically based framework for modeling the organic fractionation of sea spray aerosol from bubble film Langmuir equilibria, Atmospheric Chemistry and Physics, 14, 13 601–13 629, https://doi.org/10.5194/acp-14-13601-2014, 2014.

Burrows, S. M., Gobrogge, E., Fu, L., Link, K., Elliott, S. M., Wang, H., and Walker, R.: OCEANFILMS-2: Representing coadsorption of

10 saccharides in marine films and potential impacts on modeled marine aerosol chemistry, Geophysical Research Letters, 43, 8306–8313, https://doi.org/10.1002/2016GL069070, 2016.

Fu, P., Kawamura, K., Okuzawa, K., Aggarwal, S. G., Wang, G., Kanaya, Y., and Wang, Z.: Organic molecular compositions and temporal variations of summertime mountain aerosols over Mt. Tai, North China Plain, Journal of geophysical research, 113, 1359, 2008.

Fu, P., Kawamura, K., Kanaya, Y., and Wang, Z.: Contributions of biogenic volatile organic compounds to the formation of secondary organic

15 aerosols over Mt. Tai, Central East China, Atmospheric Environment VL -, 44, 4817–4826, 2010.

Gall, M. P., Davies-Colley, R. J., and Merrilees, R. A.: Exceptional visual clarity and optical purity in a sub-alpine lake, Limnol. Oceanogr., 58, 443–451, 2013.

Hartree, E. F.: Determination of protein: A modification of the lowry method that gives a linear photometric response, Analytical Biochemistry, 48, 422–427, 1972.

20 Laskin, A., Moffet, R. C., Gilles, M. K., Fast, J. D., Zaveri, R. A., Wang, B., Nigge, P., and Shutthanandan, J.: Tropospheric chemistry of internally mixed sea salt and organic particles: Surprising reactivity of NaCl with weak organic acids, J. Geophys. Res, 117, D15 302, https://doi.org/10.1029/2012JD017743, 2012.

Law, C. S., Woodward, E. M. S., Ellwood, M. J., Marriner, A., Bury, S. J., and Safi, K. A.: Response of surface nutrient inventories and nitrogen fixation to a tropical cyclone in the southwest Pacific, Limnol. Oceanogr., 56, 1372–1385, 2011.

25 Lowry, O. H., Rosebrough, N. J., Farr, A. L., and Randall, R. J.: Protein measurement with the Folin Phenol reagent, Journal of Biological Chemistry, 193, 265–275, 1951.

Modini, R. L., Harris, B., and Ristovski, Z.: The organic fraction of bubble-generated, accumulation mode Sea Spray Aerosol (SSA), Atmospheric Chemistry and Physics, 10, 2867–2877, 2010a.

Modini, R. L., Johnson, G. R., He, C., and Ristovski, Z. D.: Observation of the suppression of water uptake by marine particles, Atmospheric

30 Research, 98, 219–228, 2010b.

Nelson, N.: A photometric adaptation of the Somogyi method for the determination of glucose, Journal of Biological Chemistry, 153, 375–380, 1944.

Rasmussen, B. B., Nguyen, Q. T., Kristensen, K., Nielsen, L. S., and Bilde, M.: What controls volatility of sea spray aerosol? Results from laboratory studies using artificial and real seawater samples, Journal of Aerosol Science, 107, 134–141,

35 https://doi.org/10.1016/j.jaerosci.2017.02.002, 2017.

Rumble, J. R.: Physical Constants of Inorganic Compounds, in: CRC Handbook of Chemistry and Physics, CRC Press/ Taylor & Francis, Boca Raton, FL, 2018.

Safi, K. A., Brian Griffiths, F., and Hall, J. A.: Microzooplankton composition, biomass and grazing rates along the WOCE SR3 line between Tasmania and Antarctica, Deep Sea Research Part I: Oceanographic Research Papers, 54, 1025–1041, 2007.

Salter, M. E., Hamacher-Barth, E., Leck, C., Werner, J., Johnson, C. M., Riipinen, I., Nilsson, E. D., and Zieger, P.: Calcium enrichment in sea spray aerosol particles, Geophysical Research Letters, 43, 8277–8285, https://doi.org/10.1002/2016GL070275, 2016.

5   Schwier, A. N., Sellegri, K., Mas, S., Charri ere, B., Pey, J., Rose, C., Temime-Roussel, B., Jaffrezo, J. L., Parin, D., Picard, D., and et al.: Primary marine aerosol physical flux and chemical composition during a nutrient enrichment experiment in mesocosms in the Mediterranean Sea, Atmospheric Chemistry and Physics, 17, 14 645–14 660, https://doi.org/10.5194/acp-17-14645-2017, 2017.

Simoneit, B. R. T.: Composition and major sources of organic compounds of aerosol particulate matter sampled during the ACE-Asia campaign, Journal of geophysical research, 109, 995, 2004.

10   Somogyi, M.: Notes on sugar determination, Journal of Biological Chemistry, 70, 599–612, 1926.

Somogyi, M.: Notes on sugar determination, Journal of Biological Chemistry, 195, 19–23, 1952.

Zelenyuk, A., Imre, D., Cuadra-Rodriguez, L. A., and Ellison, B.: Measurements and interpretation of the effect of a soluble organic surfactant on the density, shape and water uptake of hygroscopic particles, Journal of Aerosol Science, 38, 903–923, https://doi.org/10.1016/j.jaerosci.2007.06.006, 2007.

15   Zieger, P., Väisänen, O., Corbin, J. C., Partridge, D. G., Bastelberger, S., Mousavi-Fard, M., Rosati, B., Gysel, M., Krieger, U. K., Leck, C., and et al.: Revising the hygroscopicity of inorganic sea salt particles, Nature Communications, 8, ncomms15 883, https://doi.org/10.1038/ncomms15883, 2017.

Zuend, A.: AIOMFAC (Activity Inorganic-Organic Mixtures Functional groups Activity Coefficients), https://aiomfac.lab.mcgill.ca, 2019.

Zuend, A., Marcolli, C., Luo, B. P., and Peter, T.: A thermodynamic model of mixed organic-inorganic aerosols to predict activity coefficients,
20   Atmospheric Chemistry and Physics, 8, 4559–4593, 2008.

Appendix A: Nascent SSA data

Summary of nascent SSA composition observed from chamber measurements during SOAP voyage. The three tables are the computed data from the VH-TDMA measurements, the IBA analysis of collected filter samples and the FTIR analysis.

Nascent SSA composition from VH-TDMA

Date	Sample	Depth	Depth class	Diameter	Lat	Long	Chl-a	vOVF	nvOVF	Hydrate frac	HGF ambient	HGF heated
NZST	⬜	[m]	⬜	[nm]	[°]	[°]	[mg/m^3]	⬜	⬜	⬜	⬜	⬜
15/2/12 8:05	WB1	0.1	Surface	50	44.62	174.77	0.985	0.15	0.70	0.05	2.08	2.00
17/2/12 8:02	WB4	0.1	Surface	50	44.59	174.69	1.405	0.17	0.54	0.08	1.79	2.03
18/2/12 9:16	U7505	50.0	Deep	50	44.57	174.74	0.974	0.11	0.15	0.09	2.04	2.07
18/2/12 8:04	WB5	0.1	Surface	50	44.59	174.69	1.16	0.14	0.82	0.06	1.97	2.04
19/2/12 7:30	U7506	505.5	Deep	50	44.34	175.25	NA	0.09	0.51	0.12	2.04	NA
19/2/12 7:30	U7506	2.8	Mixed	50	44.34	175.25	0.91	0.14	0.71	0.08	1.93	2.05
20/2/12 7:15	U7507	3.1	Mixed	50	45.96	173.65	0.88	NA	NA	NA	1.88	1.99
21/2/12 7:55	U7508	2.1	Mixed	50	43.74	176.97	0.67	NA	NA	NA	1.86	2.07
21/2/12 7:55	U7508	404.5	Deep	50	43.74	176.97	NA	NA	NA	NA	1.90	2.03
22/2/12 9:22	U7510	3.1	Mixed	50	43.72	-178.16	1.52	0.10	0.00	0.16	1.92	1.93
22/2/12 8:27	WB6	0.1	Surface	50	43.72	-179.86	1.53	0.09	0.30	0.15	1.86	1.91
24/2/12 13:03	WB7	0.1	Surface	50	43.59	-179.75	0.49	0.12	0.35	0.13	1.98	2.08
24/2/12 15:15	U7518	254.7	Deep	50	43.60	-179.77	NA	0.05	0.41	0.14	2.01	NA
25/2/12 14:30	U7520	11.6	Mixed	50	43.63	179.74	0.63	NA	NA	NA	1.93	1.96
26/2/12 6:52	U7521	2.5	Mixed	50	43.96	179.31	0.53	0.09	0.30	0.13	1.98	2.05
27/2/12 14:39	WB8	0.1	Surface	50	44.11	175.14	0.46	0.10	0.26	0.14	1.88	1.98
28/2/12 13:10	U7524	11.2	Mixed	50	44.54	174.87	0.29	0.10	0.29	0.13	1.97	1.99
29/2/12 8:03	WB9	0.1	Surface	50	44.60	174.87	0.45	0.09	0.10	0.15	1.84	1.94
2/3/12 14:59	U7528	9.2	Mixed	50	44.19	174.94	0.45	0.09	0.32	0.14	1.88	2.01
3/3/12 14:45	U7530	10.3	Mixed	50	44.78	174.65	0.49	0.09	0.19	0.14	1.83	1.97
3/3/12 14:45	U7530	810.5	Deep	50	44.78	174.65	NA	0.01	0.00	0.21	1.90	2.00
4/3/12 15:25	U7532	9.0	Mixed	50	44.24	174.52	1.01	0.06	0.11	0.16	1.87	1.94
5/3/12 9:04	WB10	0.1	Surface	50	44.19	174.30	NA	0.10	0.24	0.15	1.89	2.04

Nascent SSA composition from IBA

Date	Sample	Depth	Depth class	Lat	Long	Na/ Total inorg.	Mg/ Total inorg.	Cl/ Total inorg.	K / Total inorg.	Ca/ Total inorg.	Zn/ Total inorg.	Br/ Total inorg.	Sr/ Total inorg.	Sulfate/ Total inorg.	Inorganic conc.
NZST	⬚	[m]	⬚	[°]	[°]	⬚	⬚	⬚	⬚	⬚	⬚	⬚	⬚	⬚	[µg/m^3]
15/2/12 8:05	WB1	0.1	Surface	44.62	174.77	0.321	0.010	0.541	0.010	0.017	0.000	0.002	0.000	0.098	214.2
17/2/12 8:02	WB4	0.1	Surface	44.59	174.69	0.351	0.014	0.524	0.005	0.017	0.000	0.003	0.000	0.085	216.0
18/2/12 9:16	U7505	50.0	Deep	44.57	174.74	0.340	0.014	0.524	0.009	0.016	0.000	0.002	0.000	0.094	326.0
18/2/12 8:04	WB5	0.1	Surface	44.59	174.69	0.325	0.020	0.511	0.010	0.028	0.000	0.003	0.000	0.104	164.7
19/2/12 7:30	U7506	505.5	Deep	44.34	175.25	0.351	0.022	0.506	0.006	0.019	0.000	0.002	0.000	0.093	102.5
19/2/12 7:30	U7506	2.8	Mixed	44.34	175.25	0.322	0.023	0.478	0.017	0.032	0.001	0.002	0.000	0.126	58.9
20/2/12 7:15	U7507	3.1	Mixed	45.96	173.65	NA	NA	NA	NA	NA	NA	NA	NA	NA	NA
21/2/12 7:55	U7508	2.1	Mixed	43.74	176.97	NA	NA	NA	NA	NA	NA	NA	NA	NA	NA
21/2/12 7:55	U7508	404.5	Deep	43.74	176.97	NA	NA	NA	NA	NA	NA	NA	NA	NA	NA
22/2/12 9:22	U7510	3.1	Mixed	43.72	-178.16	0.343	0.014	0.532	0.005	0.020	0.000	0.002	0.000	0.083	151.3
22/2/12 8:27	WB6	0.1	Surface	43.72	-179.86	0.301	0.024	0.491	0.008	0.035	0.000	0.002	0.001	0.139	69.0
24/2/12 13:03	WB7	0.1	Surface	43.59	-179.75	0.316	0.019	0.513	0.009	0.022	0.000	0.002	0.000	0.117	187.0
24/2/12 15:15	U7518	254.7	Deep	43.60	-179.77	0.341	0.031	0.449	0.014	0.025	0.000	0.002	0.000	0.138	75.0
25/2/12 14:30	U7520	11.6	Mixed	43.63	179.74	0.418	0.001	0.470	0.012	0.024	0.000	0.003	0.000	0.072	66.6
26/2/12 6:52	U7521	2.5	Mixed	43.96	179.31	0.282	0.017	0.586	0.008	0.016	0.000	0.002	0.000	0.089	59.4
27/2/12 14:39	WB8	0.1	Surface	44.11	175.14	0.303	0.013	0.557	0.007	0.021	0.000	0.002	0.000	0.096	177.3
28/2/12 13:10	U7524	11.2	Mixed	44.54	174.87	0.312	0.011	0.554	0.008	0.019	0.000	0.002	0.000	0.095	178.6
29/2/12 8:03	WB9	0.1	Surface	44.60	174.87	0.300	0.012	0.584	0.008	0.013	0.000	0.002	0.000	0.082	304.9
2/3/12 14:59	U7528	9.2	Mixed	44.19	174.94	NA	NA	NA	NA	NA	NA	NA	NA	NA	NA
3/3/12 14:45	U7530	10.3	Mixed	44.78	174.65	0.307	0.011	0.578	0.006	0.016	0.000	0.002	0.000	0.079	428.5
3/3/12 14:45	U7530	810.5	Deep	44.78	174.65	0.332	0.008	0.570	0.006	0.009	0.000	0.002	0.000	0.072	163.6
4/3/12 15:25	U7532	9.0	Mixed	44.24	174.52	0.303	0.015	0.555	0.009	0.022	0.000	0.002	0.000	0.093	388.4
5/3/12 9:04	WB10	0.1	Surface	44.19	174.30	0.263	0.017	0.584	0.015	0.023	0.000	0.000	0.000	0.098	221.4

Nascent SSA composition from FTIR

Date	Sample	Depth	Depth class	Lat	Long	Chl-a	Alcohol/ Total OM	Alkane/ Total OM	Carbonyl/ Total OM	Amine/ Total OM	Acid/ Total OM	Total OM	OMF
NZST	🔲	[m]	🔲	[°]	[°]	[mg/m^3]	🔲	🔲	🔲	🔲	🔲	🔲	[µg/m^3]
15/2/12 8:05	WB1	0.1	Surface	44.62	174.77	0.985	0.722	0.093	0.000	0.140	0.044	45.29	0.17
17/2/12 8:02	WB4	0.1	Surface	44.59	174.69	1.405	0.773	0.102	0.000	0.077	0.047	54.08	0.20
18/2/12 9:16	U7505	50.0	Deep	44.57	174.74	0.974	0.757	0.114	0.000	0.128	0.000	16.29	0.05
18/2/12 8:04	WB5	0.1	Surface	44.59	174.69	1.16	0.820	0.054	0.000	0.101	0.025	42.18	0.20
19/2/12 7:30	U7506	505.5	Deep	44.34	175.25	NA	0.770	0.118	0.000	0.112	0.000	14.83	0.13
19/2/12 7:30	U7506	2.8	Mixed	44.34	175.25	0.91	0.619	0.155	0.000	0.122	0.104	17.84	0.23
20/2/12 7:15	U7507	3.1	Mixed	45.96	173.65	0.88	NA	NA	NA	NA	NA	NA	NA
21/2/12 7:55	U7508	2.1	Mixed	43.74	176.97	0.67	NA	NA	NA	NA	NA	NA	NA
21/2/12 7:55	U7508	404.5	Deep	43.74	176.97	NA	NA	NA	NA	NA	NA	NA	NA
22/2/12 9:22	U7510	3.1	Mixed	43.72	-178.16	1.52	0.800	0.094	0.000	0.106	0.000	15.89	0.10
22/2/12 8:27	WB6	0.1	Surface	43.72	-179.86	1.53	0.741	0.134	0.000	0.125	0.000	11.90	0.15
24/2/12 13:03	WB7	0.1	Surface	43.59	-179.75	0.49	0.712	0.112	0.000	0.116	0.061	26.76	0.13
24/2/12 15:15	U7518	254.7	Deep	43.60	-179.77	NA	0.705	0.154	0.000	0.141	0.000	9.85	0.12
25/2/12 14:30	U7520	11.6	Mixed	43.63	179.74	0.63	0.855	0.072	0.000	0.073	0.000	13.21	0.17
26/2/12 6:52	U7521	2.5	Mixed	43.96	179.31	0.53	0.726	0.143	0.000	0.131	0.000	3.67	0.06
27/2/12 14:39	WB8	0.1	Surface	44.11	175.14	0.46	0.810	0.087	0.000	0.103	0.000	23.38	0.12
28/2/12 13:10	U7524	11.2	Mixed	44.54	174.87	0.29	0.709	0.115	0.000	0.133	0.043	10.60	0.06
29/2/12 8:03	WB9	0.1	Surface	44.60	174.87	0.45	0.739	0.107	0.000	0.082	0.072	9.18	0.03
2/3/12 14:59	U7528	9.2	Mixed	44.19	174.94	0.45	NA	NA	NA	NA	NA	NA	NA
3/3/12 14:45	U7530	10.3	Mixed	44.78	174.65	0.49	0.849	0.101	0.000	0.051	0.000	16.50	0.04
3/3/12 14:45	U7530	810.5	Deep	44.78	174.65	NA	0.783	0.102	0.000	0.082	0.034	6.24	0.04
4/3/12 15:25	U7532	9.0	Mixed	44.24	174.52	1.01	0.746	0.086	0.000	0.118	0.050	50.30	0.11
5/3/12 9:04	WB10	0.1	Surface	44.19	174.30	NA	0.829	0.050	0.000	0.097	0.024	29.91	0.12